IEEE Access
Multidisciplinary | Rapid Review | Open Access Journal

Received May 20, 2017, accepted June 2, 2017, date of publication June 6, 2017, date of current version June 27, 2017.

Digital Object Identifier 10.1109/ACCESS.2017.2712616

A Novel Planar Printed Dual-Band Magneto-Electric Dipole Antenna

CHEN-YANG SHUAI, (Student Member, IEEE), AND GUANG-MING WANG
Air Force Engineering University, Xi'an 710051, China
Corresponding author: Guang-Ming Wang (wgming01@sina.com)

ABSTRACT In this paper, a novel planar printed dual-band magneto-electric dipole antenna is proposed. The proposed antenna is composed of a conventional bow-tie patch as an electric dipole, a semi-circular loop that operates as a magnetic dipole, a coplanar ground plane, and a wideband microstrip-to-coplanar-stripline transition balun. By etching a pair of complementary capacitively loaded loop slots on the bow-tie radiation patch, a notched band is introduced to form the dual-band antenna. And a coplanar ground is adopted to make the entire antenna become a planar printed structure. Additionally, the proposed antenna loads the periodical interdigital capacitance structure on the semi-circular loop for the purpose of making the current flowing along the loop maintain the same phase and improving the performances of the magnetic dipole. The proposed antenna was fabricated and measured. The measured results keep in good accordance with the simulated ones. Consequently, the proposed antenna achieves a dual-band operation at 2.37∼2.82 GHz (17.3%) and 3.14∼4.10 GHz (26.5%) with the Voltage Standing Wave Ratio (VSWR) less than 2, so it can be applied for WLAN (2.4–2.484 GHz) and WiMAX (2.5–2.69 GHz/3.4–3.69 GHz). Meanwhile, the stable gain, symmetrical, and stable unidirectional radiation patterns, low cross polarization, and low back lobe are also obtained at the dual bands.

INDEX TERMS Planar printed, dual-band, magneto-electric dipole, complementary capacitively loaded loop (CCLL), interdigital capacitance (IDC).

I. INTRODUCTION

With the fast development of the wireless communication technologies, the wideband or multiband antennas are in good need to satisfy the increasing number of service bands, especially the WLAN, WiMAX, and LTE operating frequency bands. Compared with the conventional single band antenna, the multiband antenna can effectively decrease the number of the antenna elements and covering areas. Therefore, the multiband antenna has become a research hotspot. Recently, lots of dual- and triple-band antennas have been proposed in some open literatures [1]–[4].

To achieve multiple bands, the most general method is to etch various slots on the radiation patch or ground plane. In literatures [5], [6], the proposed antennas obtain multiple bands by etching slots on the monopole antennas. The second method is to get the antennas with different operating frequency bands together to obtain multiple bands [2]–[4]. However, this type of method is relatively complicated, due to additional matching circuits. The third method is to add the strips on the slot antenna to achieve multiple bands [7], [8]. Furthermore, in the fourth method, the antennas obtain multiple bands by introducing various band-notched structures [9]–[11]. Except for four types of conventional methods above, recently, the unit cell of the metamaterials is also widely utilized for multiband antenna design and soon the multiband antennas by loading the unit cell of metamaterials become a research hotspot. In [12] and [13], by introducing the complementary split-ring resonator (CSRR) which is a common unit cell of magnetic metamaterials, the ultra-wideband antennas obtain multiple stopbands. In [14], the proposed antenna adopts another unit cell of magnetic metamaterials named as capacitively loaded loop (CLL) to form multiple operating frequency bands. These unit cells of magnetic metamaterials have many advantages over the conventional methods. For example, they have compact structure and the inspired stopbands by them cannot almost affect the other operating frequency bands. Moreover, metamaterials can also be used for increasing the antenna gain as shown in [15]. However, most of the multiband antennas above are monopoles, so the applications of these antennas are limited in some respects. Instead, dipole antenna can satisfy the higher demands for multiband wireless communication.

In 2006, based on the concept of the complementary antennas, Luk proposed a new magneto-electric (ME) dipole antenna [16]. Over the operating frequency band, this type of antenna has not only broad bandwidth, simple structure, stable gain, low cross polarization, and wide half power beamwidth, but also the identical radiation patterns of E-plane and H-plane. Due to the notable advantages of the ME dipole antenna, many researchers have applied it to multiband antenna design and made some progress. In [17], by adopting the U-shaped electric dipole, the designed ME dipole antenna achieves dual-band operation. In [18], the proposed antenna utilizes a dual-layer cross-magneto-electric (ME)-dipole structure to obtain a dual-band operation. Though these dual-band ME dipole antennas achieve better electrical characteristics compared with conventional multiband antennas, they both have the bulky three-dimensional structure, especially the large reflector. This drawback makes the dual-band ME dipole antennas become uneasy installation and unsuitable for mass production. Therefore, the practical applications of the dual-band ME dipole antennas above are restricted.

In order to solve these problems above, in this paper, a novel planar printed dual-band ME dipole antenna is proposed. By etching a pair of complementary capacitively loaded loop (CCLL) slots on the bow-tie radiation patch, a notched band is generated to form a dual-band operation for WLAN and WiMAX applications. Additionally, the proposed ME dipole antenna utilizes a coplanar ground to achieve a planar printed structure. Meanwhile, for improving the performances of the magnetic dipole, the periodical interdigital capacitance (IDC) structure is introduced to make the current flowing along the loop maintain the same phase. Finally, the proposed antenna obtains good electrical characteristics and the measured results keep in good accordance with the simulated ones. It is demonstrated that the proposed dual-band ME dipole antenna can be installed easily and suitable for mass production. Meanwhile, the antenna is also a good candidate for the multiband wireless communication.

II. ANTENNA DESIGN

The geometry of the proposed antenna is shown in Fig.1(a)-(c). The overall size of the antenna is $W \times L \times d$. And the proposed antenna is printed on the single-layer Duroid 5880 dielectric substrate with the permittivity of 2.2 and thickness of 0.78mm. From the pictures, it can be seen that the proposed antenna is composed of a conventional bow-tie radiation patch, a semi-circular loop, a coplanar ground, and a microstrip-to-coplanar-stripline (CPS) transition balun.

Fig.1(a) depicts the top view of the proposed antenna. The bow-tie patch is adopted to work as an electric dipole and the flare angle named as θ is chosen to be 64° for wideband impedance matching. And the width g of the slot between bow-tie patch is also an important parameter for impedance matching. By using Ansoft HFSS, g is optimized and chosen to be 4mm. Additionally, a semi-circular loop is introduced

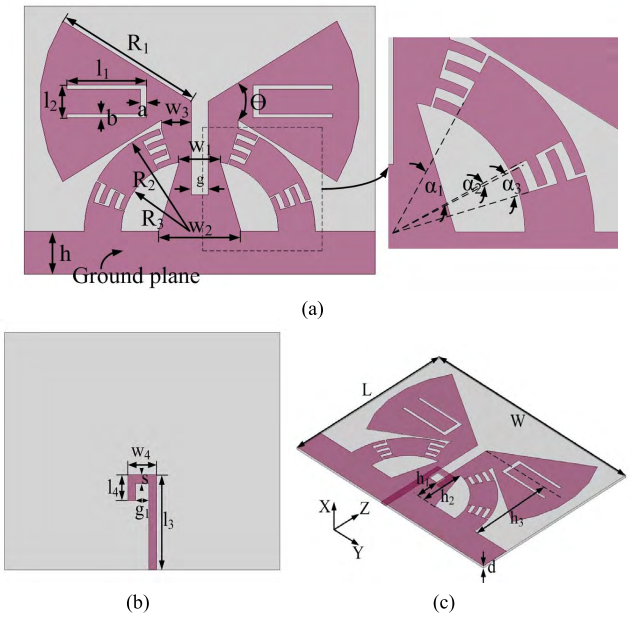

FIGURE 1. The geometry of the proposed antenna: (a) top view; (b) bottom view; (c) perspective view.

to operate as a magnetic dipole together with the ground between the loop. Furthermore, to improve the performance of the magnetic dipole, the periodical interdigital capacitance is loaded on the semi-circular loop. As is known to us, the value of the interdigital capacitance depends on the number of the fingers. When the number of the fingers is designed precisely, the semi-circular loop is equivalent to composite right/left-handed transmission line (CRLH TL) and the current flowing along the loop maintains the same phase. By simulated analysis, the number of the fingers is chosen to be four. In this paper, instead of using a large vertical ground plane, a small-size coplanar ground is adopted to help the antenna achieve a planar printed structure. As a result, the planar printed antenna is easily fabricated and suitable for mass production. For the purpose of good impedance matching, we utilize a wideband microstrip-to-coplanar-stripline (CPS) transition balun to couple the electromagnetic energy to the radiation portion. Fig.1(b) shows the bottom view of the antenna. It can be seen that Γ-shaped strip feeding structure is printed on the back of the substrate. And the width of the Γ-shaped strip is finally determined to be 2.4mm for achieving the 50Ω characteristic impedance. Meanwhile, a SMA connector is connected to the Γ-shaped strip for transmitting the exciting signals.

In order to obtain a dual-band operation, a pair of CCLL slots is etched on the bow-tie patch. Consequently, the CCLL slots generate a notched band. And the notched frequency of the resonant mode of the CCLL slots is able to be approximately expressed by the following formulas [14]:

$$f_{notch} \approx \frac{c}{2L_{CCLL}\sqrt{\varepsilon_{eff}}} \tag{1}$$

TABLE 1. Dimensions of the proposed antenna.

Parameters	W	L	R_1	R_2	R_3	w_1
Values/mm	85	65	36.8	26	17	10
Parameters	w_2	w_3	w_4	l_1	l_2	l_3
Values/mm	20	7.25	8.8	19.3	8	26
Parameters	l_4	h	h_1	h_2	h_3	a
Values/mm	7	10.4	8.8	16.8	31.5	1.5
Parameters	b	g	g_1	s	d	
Values/mm	1	4	4	2.3	0.78	
Parameters	α_1	α_2	α_3	θ		
Values	33°	1°	11°	64°		

(a) (b)

FIGURE 2. The prototype of the proposed antenna: (a) top view; (b) bottom view.

$$\varepsilon_{eff} = \frac{1 + \mathrm{Re}(\varepsilon_r)}{2} \tag{2}$$

$$L_{CCLL} = 2l_1 + l_2 \tag{3}$$

Where c represents the speed of the light, L_{CCLL} represents the total length of the CCLL slots, and ε_{eff} represents the effective permittivity. Compared with the conventional multi-band technologies, loading CCLL slots has little impact on electrical characteristics of the antenna at other frequency bands and the notched band inspired by the CCLL slots is easily adjusted.

All the dimensions of the proposed antenna in detail are shown in Table I.

III. ANTENNA PERFORMANCE

The prototype of the proposed antenna is shown in Fig.2(a)-(b). The simulated results are obtained by using Ansoft HFSS. And the measured results are obtained by vector network analyzer and anechoic chamber.

A. EVOLUTION PROCESS

Fig.3 depicts the evolution process of the proposed antenna. The original antenna named as antenna I is shown in Fig.3(a). Based on antenna I, antenna II shown in Fig.3(b) is achieved by loading the periodical interdigital capacitance structure on the semi-circular loop. Furthermore, the proposed antenna shown in Fig.3(c) adds a pair of CCLL slots on the bow-tie patch. The simulated and measured VSWRs and gains of the three antennas above are depicted in Fig.4. We can

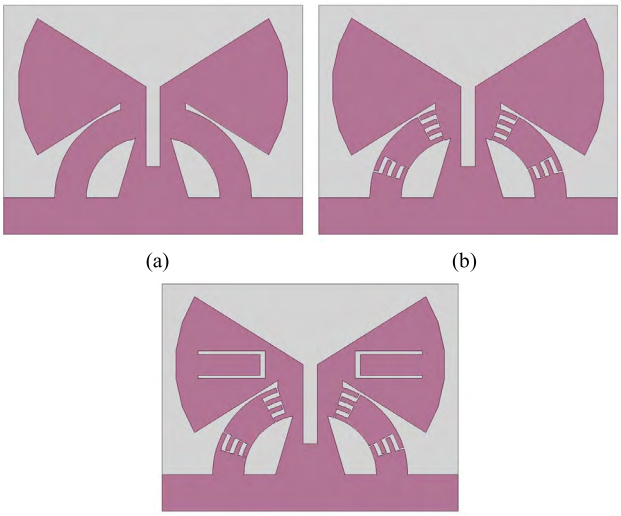

(a) (b) (c)

FIGURE 3. The evolution process of the proposed antenna: (a) antenna I; (b) antenna II; (c) the proposed antenna.

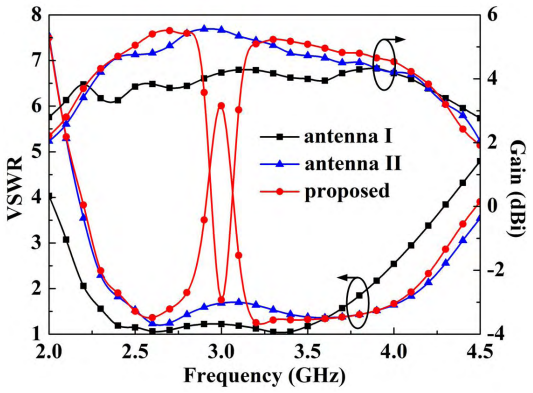

FIGURE 4. The simulated VSWRs and gains of the three antennas.

see that antenna I obtains a broad impedance bandwidth of 54.5% from 2.20GHz to 3.85GHz with the VSWR less than 2, and the antenna II also obtains a broad impedance bandwidth of 55.4% from 2.35GHz to 4.15GHz. But the periodical interdigital capacitance structure makes the operating frequency band of antenna II move to higher frequency. In addition, by etching CCLL slots, the notched frequency (3GHz) is generated to achieve a dual-band operation at 2.37∼2.82GHz (17.3%) and 3.14∼4.10GHz (26.5%) with the VSWR less than 2, which is suitable for WLAN (2.4-2.484GHz) and WiMAX (2.5-2.69GHz/3.4-3.69GHz) applications. It is worth noting that at the notched frequency, the VSWR reaches 6 and the proposed antenna obtains a good band-notched characteristic. On the other hand, we can also see that compared with antenna I, antenna II obtains higher gain from 4.2dBi to 5.5dBi due to the function of the interdigital capacitance over the operating frequency band. Finally, the simulated stable gains of the proposed antenna are 4.3∼5.5dBi and 4.2∼5.2dBi at the dual bands. Meanwhile,

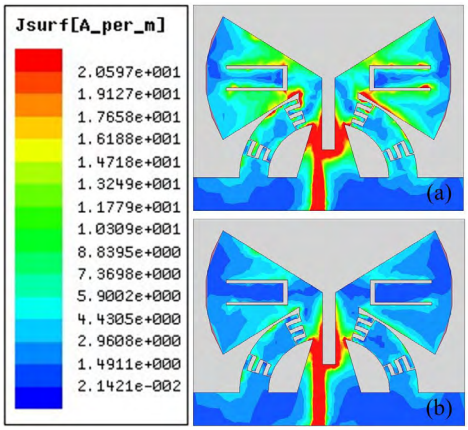

FIGURE 5. Surface current distributions for the proposed antenna over a period of time at 2.6GHz: (a) $t = 0$ ($T/2$); (b) $t = T/4$ ($3T/4$).

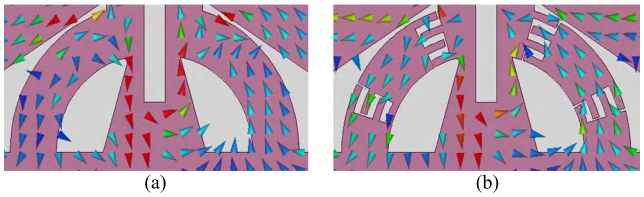

FIGURE 6. The vector current distributions for the antennas with/without interdigital capacitance at 2.6GHz: (a) without the interdigital capacitance; (b) with the interdigital capacitance.

it is also demonstrated that the introduction of the notched band inspired by CCLL slots has little impact on the performances of the antenna at other operating frequency bands.

B. CURRENT ANALYSIS

To explain the principle of the proposed dual-band ME dipole antenna further, the surface current distributions over a period of time T at 2.6GHz are illustrated in Fig.5(a)-(b). At $t = 0$ and $T/2$, the maximum of the surface current appears on the surface of the bow-tie radiation patch. So an electric dipole mode is generated at $t = 0$ and $T/2$. Furthermore, when $t = T/4$ and $3T/4$, the maximum of the surface current appears on the surface of the semi-circular loop. Therefore, a magnetic dipole mode is excited at $t = T/4$ and $3T/4$. The results above clearly illustrate that two types of radiation modes have a phase shift of 90°. As a result, the phase shift of 90° can counteract the inherent phase shift between an electric dipole and a magnetic dipole. Therefore an electric dipole and a magnetic dipole are excited simultaneously, and a ME dipole with complementary characteristics is achieved.

Fig.6(a)-(b) illustrate the vector current distributions for the antennas with and without the interdigital capacitance at 2.6GHz. By a comparison, it is obvious that the vector current flowing along the loop with the interdigital capacitance maintains the same phase, whereas the vector current flowing along the loop without the interdigital capacitance is relatively littery. The reason causing the difference is

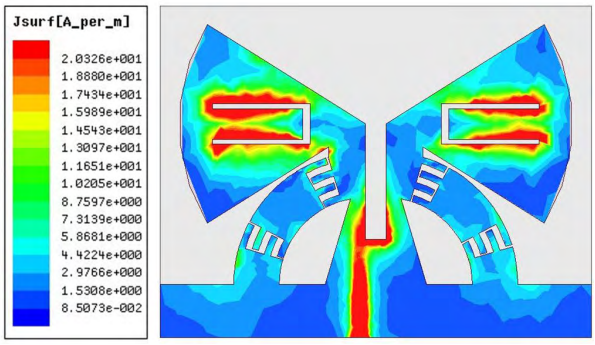

FIGURE 7. Surface current distribution for the proposed antenna at the notched frequency (3GHz).

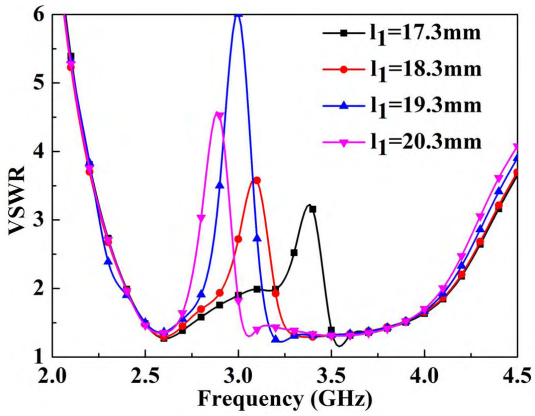

FIGURE 8. The simulated VSWRs with different lengths of l_1.

mainly because the semi-circular loop with the interdigital capacitance is equivalent to composite right/left-handed transmission line (CRLH TL). Fig.7 depicts the surface current distribution for the proposed antenna at the notched frequency (3GHz). When the proposed antenna works at 3 GHz, the resonant mode of the CCLL slots is excited and the maximum of the surface current is located on the CCLL slots. In other words, the electromagnetic energy is stored on the CCLL slots and cannot radiate outward.

C. PARAMETER ANALYSIS

In this portion, we select several important parameters of CCLL slots to analyse the performances of the antenna. Fig.8 depicts the simulated VSWRs with different lengths of l_1. From the picture, it is seen that as the l_1 increases, the current path on the CCLL slots is extended and the notched frequency of the resonant mode of the CCLL slots moves to lower frequency. But we can also found that the other operating frequency bands are not almost affected. Therefore, the notched frequency can be adjusted independently. Fig.9 shows the simulated VSWRs with different lengths of l_2. As l_2 increases, the notched frequency also moves to lower frequency. But the extent of the changes is not as large as the former. It is demonstrated that the

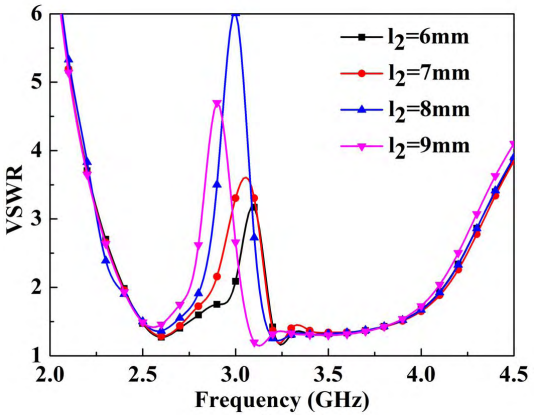

FIGURE 9. The simulated VSWRs with different lengths of l_2.

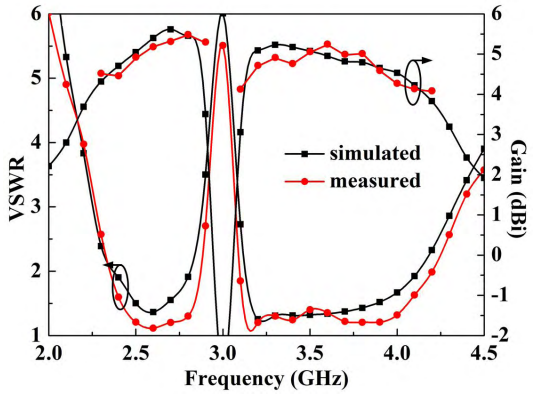

FIGURE 10. The simulated and measured VSWRs and gains of the proposed antenna.

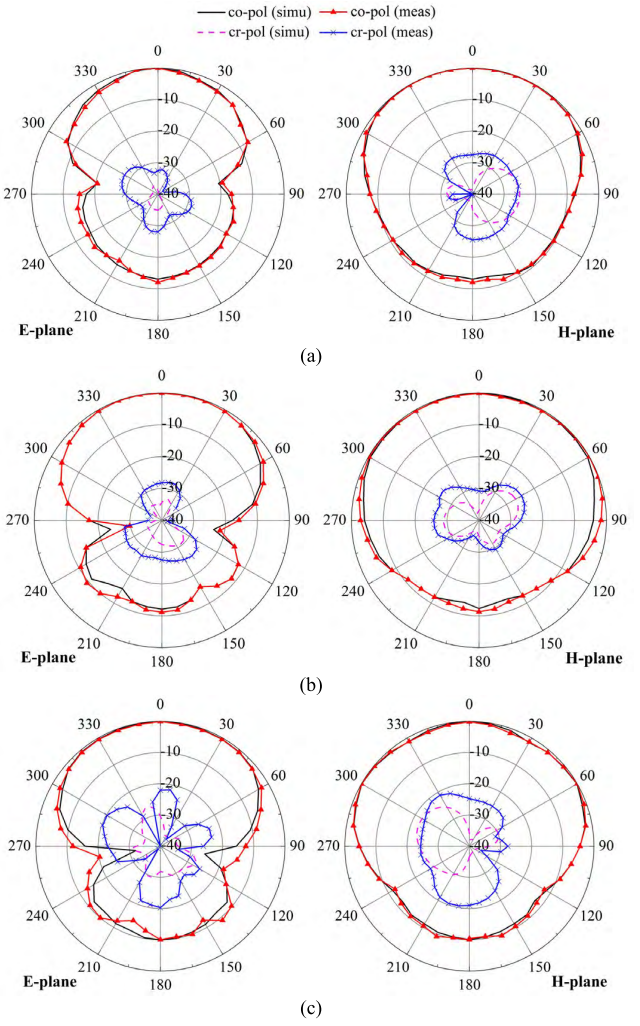

FIGURE 11. The simulated and measured radiation patterns of the proposed antenna: (a) at 2.6GHz; (b) 3.3GHz; (c) 4.0GHz.

notched frequency is more sensitive to l_1. According to formulas (1)-(3) and optimizing analysis, we finally select 3GHz as the notched frequency. Correspondingly, l_1 and l_2 are determined to be 19.3mm and 8mm. Therefore, the proposed antenna obtains a notched band from 2.82GHz to 3.14GHz.

D. MEASURED RESULTS

The simulated and measured VSWRs and gains of the proposed antenna are shown in Fig.10. The measured dual operating frequency bands are 2.35∼2.90GHz (20.9%) and 3.08∼4.21GHz (31.0%) with VSWR less than 2, which are suitable for WLAN(2.4-2.484GHz) and WiMAX (2.5-2.69GHz/3.4-3.69GHz) applications. Furthermore, the measured gains at the dual operating frequency bands are 4.4∼5.4dBi and 4.1∼5.2dBi. Therefore the proposed antenna achieves a dual-band operation and obtains stable gains at the dual operating frequency bands. The simulated results are in good accordance with the measured ones. However, there still exist some slight discrepancies between simulated and measured results, mainly due to measurement error, imperfect soldering, and fabrication tolerance.

Fig.11 shows the simulated and measured radiation patterns of the proposed antenna at 2.6GHz, 3.3GHz, and 4.0GHz. The simulated results keep in good consistency with the measured ones. The proposed dual-band ME dipole antenna achieves stable and symmetrical unidirectional radiation patterns at the dual bands. Additionally, at the dual bands, low cross polarization, low back lobe and wide beamwidth are also obtained. We can see that the value of simulated cross polarization level is less than −22dB and the measured result is less than −20dB. Meanwhile, the values of measured and simulated back lobe level are both less than −10dB.

IV. CONCLUSION

In this paper, a novel planar printed dual-band ME dipole antenna is presented. By etching a pair of CCLL slots, the antenna obtains a dual-band operation at 2.37∼2.82GHz (17.3%) and 3.14∼4.10GHz (26.5%) for WLAN and WiMAX applications. And for improving the performances of the magnetic dipole, the antenna adopts the periodical interdigital capacitance structure to make the current flowing along the loop maintain the same phase. Additionally,

by utilizing a coplanar ground, the proposed antenna achieves a planar printed structure. Therefore, the antenna can be fabricated easily and is suitable for mass production. At all operating frequency bands, the proposed antenna obtains the stable gains, symmetrical and stable unidirectional radiation patterns, low cross polarization, and low back lobe. With these advantages above, the proposed antenna is a good candidate for multiband wireless communication.

REFERENCES

[1] X. L. Sun, L. Liu, S. W. Cheung, and T. I. Yuk, "Dual-band antenna with compact radiator for 2.4/5.2/5.8 GHz WLAN applications," *IEEE Trans. Antennas Propag.*, vol. 60, no. 12, pp. 5924–5931, Dec. 2012.

[2] C.-J. Wang and K.-L. Hsiao, "CPW-fed monopole antenna for multiple system integration," *IEEE Trans. Antennas Propag.*, vol. 62, no. 2, pp. 1007–1011, Feb. 2014.

[3] S. Verma and P. Kumar, "Compact triple-band antenna for WiMAX and WLAN applications," *Electron. Lett.*, vol. 50, no. 7, pp. 484–486, Mar. 2014.

[4] J. Soler, F. J. González, C. Puente, and J. Anguera, "Advances in loading techniques to design multifrequency monopole antennas," *Microw. Opt. Technol. Lett.*, vol. 41, no. 6, pp. 434–437, Jun. 2004.

[5] K. L. Wong and L. C. Lee, "Multiband printed monopole slot antenna for WWAN operation in the laptop computer," *IEEE Trans. Antennas Propag.*, vol. 57, no. 2, pp. 324–330, Feb. 2009.

[6] Y. Xu, Y.-C. Jiao, and Y.-C. Luan, "Compact CPW-fed printed monopole antenna with triple-band characteristics for WLAN/WiMAX applications," *Electron. Lett.*, vol. 48, no. 24, pp. 1519–1520, Nov. 2012.

[7] W. S. Chen and K. Y. Ku, "Band-rejected design of the printed open slot antenna for WLAN/WiMAX operation," *IEEE Trans. Antennas Propag.*, vol. 56, no. 4, pp. 1163–1169, Apr. 2008.

[8] L. Dang, Z. Y. Lei, Y. J. Xie, G. L. Ning, and J. Fan, "A compact microstrip slot triple-band antenna for WLAN/WiMAX applications," *IEEE Antennas Wireless Propag. Lett.*, vol. 9, pp. 1178–1181, 2010.

[9] R. Azim, M. T. Islam, J. S. Mandeep, and A. T. Mobashsher, "A planar circular ring ultra-wideband antenna with dual band-notched characteristics," *J. Electromagn. Waves Appl.*, vol. 26, nos. 14–15, pp. 2022–2032, 2012.

[10] M. Akbari, "A new slot antenna with triple stop-band performance for UWB applications," *Microw. Opt. Technol. Lett.*, vol. 55, no. 10, pp. 2350–2354, 2013.

[11] M. Akbari, S. Zarbakhsh, and M. Marbouti, "A novel UWB antenna with dual-stopband characteristics," *Microw. Opt. Technol. Lett.*, vol. 55, no. 11, pp. 2741–2745, 2013.

[12] H. Kang and S. Lim, "Electrically small dual-band reconfigurable complementary split-ring resonator (CSRR)-loaded eighth-mode substrate integrated waveguide (EMSIW) antenna," *IEEE Trans. Antennas Propag.*, vol. 62, no. 5, pp. 2368–2373, May 2014.

[13] D. Sarkar, K. V. Srivastava, and K. Saurav, "A compact microstrip-fed triple band-notched UWB monopole antenna," *IEEE Antennas Wireless Propag. Lett.*, vol. 13, pp. 396–399, 2014.

[14] C.-C. Lin, P. Jin, and R. W. Ziolkowski, "Single, dual and tri-band-notched ultrawideband (UWB) antennas using capacitively loaded loop (CLL) resonators," *IEEE Trans. Antennas Propag.*, vol. 60, no. 1, pp. 102–109, Jan. 2012.

[15] K. L. Chung and S. Kharkovsky, "Metasurface-loaded circularly-polarised slot antenna with high front-to-back ratio," *Electron. Lett.*, vol. 49, no. 16, pp. 979–981, Aug. 2013.

[16] K. M. Luk and H. Wong, "A new wideband unidirectional antenna element," *Int. J. Microw. Opt. Technol.*, vol. 1, no. 1, pp. 35–44, Jun. 2006.

[17] K. He, S.-X. Gong, and F. Gao, "A wideband dual-band magneto-electric dipole antenna with improved feeding structure," *IEEE Antennas Wireless Propag. Lett.*, vol. 13, pp. 1729–1732, 2014.

[18] B. Feng, W. An, S. Yin, L. Deng, and S. Li, "Dual-wideband complementary antenna with a dual-layer cross-ME-dipole structure for 2G/3G/LTE/WLAN applications," *IEEE Antennas Wireless Propag. Lett.*, vol. 14, pp. 626–629, 2015.

[19] K. L. Chung, T. H. Mak, and W. Y. Tam, "A modified two-strip monopole antenna for WiFi and WiMAX applications," *Microw. Opt. Technol. Lett.*, vol. 51, no. 12, pp. 2884–2886, Dec. 2009.

[20] P. W. Chan, H. Wong, and E. K. N. Yung, "Unidirectional antenna composed of dipole and loop," *Electron. Lett.*, vol. 43, no. 22, pp. 1176–1177, Oct. 2007.

[21] X. T. Wu, W. J. Lu, J. Xu, K. F. Tong, and H. B. Zhu, "Loop-monopole composite antenna for dual-band wireless communications," *IEEE Antennas Wireless Propag. Lett.*, vol. 14, pp. 293–296, 2015.

[22] H. W. Lai and H. Wong, "Substrate integrated magneto-electric dipole antenna for 5G Wi-Fi," *IEEE Trans. Antennas Propag.*, vol. 63, no. 2, pp. 870–874, Feb. 2015.

[23] W. J. Lu, J. W. Shi, K. F. Tong, and H. B. Zhu, "Planar endfire circularly polarized antenna using combined magnetic dipoles," *IEEE Antennas Wireless Propag. Lett.*, vol. 14, pp. 1263–1266, 2015.

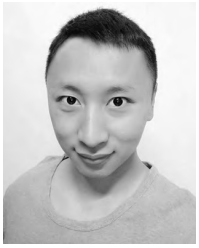

CHEN-YANG SHUAI (S'15) was born in China in 1992. He received the B.S. degree in control engineering from Air Force Engineering University, Xi'an, China, in 2015, where he is currently pursuing the M.S. degree in electromagnetic field and microwave technology.

His research interests include microwave circuits, antenna array, and gradient metasurfaces.

GUANG-MING WANG was born in China in 1964. He received the B.S. and M.S. degrees from Air Force Engineering University, Xi'an, China, in 1982 and 1990, respectively, and the Ph.D. degree from the University of Electronic Science and Technology, Chengdu, China, in 1994, all in electromagnetic field and microwave technology.

He joined Air Force Engineering University as an Associate Professor, was promoted to a Full Professor in 2000, and is currently the Head of the Microwave Laboratory. He has authored or co-authored over 150 conference and journal papers. His current interests include microwave circuits, antennas, and also the new structures, including EBG, PBG, metamaterials, and fractals.

Dr. Wang has been a Senior Member of the Chinese Commission of Communication and Electronic. From 1994 to date, he received and warranted several items supported under the National Natural Science Foundation of China and fulfilled many local scientific research programs.